# NJC

## Accepted Manuscript

This article can be cited before page numbers have been issued, to do this please use: L. Satish, S. Millan, K. bera, S. Mahapatra and H. Sahoo, *New J. Chem.*, 2017, DOI: 10.1039/C7NJ02900D.




ROYAL SOCIETY OF CHEMISTRY

rsc.li/njc

View Article Online
DOI: 10.1039/C7NJ02900D

# A Spectroscopic and Molecular dynamic simulation approach towards the stabilizing effect of ammonium based Ionic Liquids on Bovine serum albumin

Lakkoji Satish, Sabera Millan, Krishnendu Bera, Sujata Mohapatra, and Harekrushna Sahoo*

*Department of Chemistry, National Institute of Technology Rourkela, Odisha, 769008, India

* Corresponding Address:
Dr. Harekrushna Sahoo
Department of Chemistry
National Institute of Technology
Rourkela-769008
Sundergarh, Odisha
Email: sahooh@nitrkl.ac.in
Phone: +91 6612462665

**Abstract -** In this article, we have explored the impact of ammonium based ionic liquid (IL) on the thermal unfolding/refolding of Bovine serum albumin (BSA) in aqueous solutions using thermal circular dichroism (CD) spectroscopy and molecular dynamic simulation studies. In the attempt of searching ILs which can stabilize BSA at higher temperatures, we found good results with ammonium based IL. Our results show that the hydrophobicity of the IL is very crucial in the refolding phenomenon. More hydrophobic IL, triethylhexylammonium bromide shows better refolding of thermally denatured BSA and the stabilization is found to be dependent on the concentration of IL. Moreover, fluorescence measurements (synchronous, life time, 8-Anilino-1-naphthalenesulfonic Acid (ANS)) were used to decipher the conformational changes of protein in the IL medium. The spectroscopic studies suggest that native state of BSA is not altered in the IL medium rather a compact structure of BSA is established which is further supported by the molecular dynamic simulation analysis. In addition, the esterase like activity of BSA was studied in the IL medium and the possible binding sites were investigated using a molecular docking program. We hope the present study is successful in interpreting the possible mechanism of interaction between BSA and ILs as well as the stabilizing/destabilizing effect of ILs on BSA.

**Keywords** – Ionic liquids, Bovine serum albumin, Circular dichroism, Molecular dynamic simulation

View Article Online
DOI: 10.1039/C7NJ02900D



## Introduction

Stability of proteins in the aqueous medium is important in various fields such as medicine, pharmacy, biochemistry, and food industry. The stability of the protein primarily depends on the interaction of the protein with its surrounding medium (solvent). Any changes from their native environment make the protein denatured. Most of these interactions are nonbonded such as hydrogen bonding, electrostatic, and hydrophobic interactions.

Proteins denature in extreme conditions like very high/low temperatures, pressure, strong acidic/basic conditions, high salt concentration etc. Therefore, keeping the protein in native form in above mentioned stress conditions is of primary importance in biological fields. Researchers have developed many co-solvents which can stabilize the proteins. For example, sugars and polyhydric alcohol are reported to act as strong stabilizers for proteins.[1-3] Another group of stabilizers, i.e., Ionic liquids (ILs), emerged as a new class of compatible solvents for biomolecules.[4-7] ILs are more advantageous as compared to common solvents as they have some unique features like negligible vapour pressure, high ionic conductivity, low toxicity, the absence of flammability and high variability (tuned by changing cation and anion).[8, 9] These properties make ILs availed in various fields including electrochemistry, drug delivery, polymer chemistry, biosensing, pharmaceutical and many more. Moreover, ILs were reported to be an effective biocompatible media, which able to increase protein activity, refolding and yield in comparison to other solvent medium.[10-13]

The number of research articles publishing relating to the behaviour of proteins in the IL medium has been increased in recent years. Those studies are related to the stability of the protein in an aqueous solution of IL or in neat ILs. These studies show that the behaviour of proteins in ILs does not depend on a common rule. It is evidenced from the literature that the protein stability depends on the protein as well as on the composition of ILs.

From the literature, it was found that ammonium-based ILs act as good stabilizing cosolvent for proteins because of their water like properties.[14] These ILs are able to stabilize proteins as well as are good at protein refolding. Here, we are presenting some of the studies showing the stabilizing and refolding ability of ILs. Attri, P et al. revealed that triethyl ammonium salts are better-refolding additives as compared to imidazolium-based ILs for α-chymotrypsin in thermally denatured conditions.[15] Recently, the refolding ability of ammonium based ILs with fixed $[NTf_2]^-$ anion on urea denaturation of lysozyme was reported.[16] It was found that triethylammonium methane sulfonate was able to refold 97% of thermally denatured lysozyme and a work by Byrne showed that the Ethylammonium nitrate efficiently dissolves the lysozyme fibrils.[11, 17] Moreover, different ammonium based ILs were reported to have a stabilizing effect on different proteins like lysozyme[18, 19], α-chymotrypsin[20], cyt c[21], Succinyl concanavalin A[22], Laccase[23], insulin[24]. In contrast, there were reports revealing the destabilizing effect of some ammonium based ILs on different proteins. These observations give a contradictory statement regarding the role of ILs on the stabilization and destabilization of proteins. There is no particular rule which can depict the role of ILs on biomolecules. Therefore, more detailed investigation is done by considering different ILs on Bovine serum albumin (BSA) to elucidate a better interaction mechanism which can be helpful in selection of ILs in biochemical field. Herein, specifically, we reported the effect of different cation moiety of ammonium based IL on the reversible thermal unfolding/refolding of BSA.

View Article Online
DOI: 10.1039/C7NJ02900D



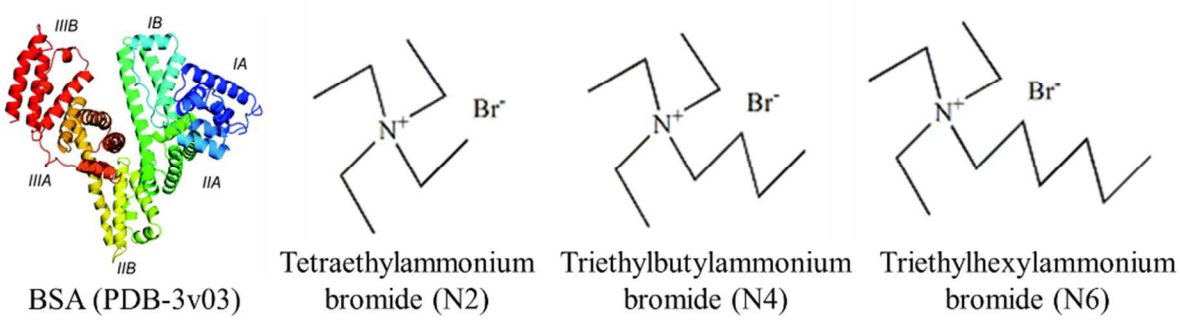


BSA (PDB-3v03) | Tetraethylammonium bromide (N2) | Triethylbutylammonium bromide (N4) | Triethylhexylammonium bromide (N6)

**Scheme 1**. Structural representation of BSA and ammonium-based ILs employed in this study.

From the literature survey as well as our previous work, we observed that the concentration of ILs has a great impact on protein structure and stability. [25, 26] [25, 26] [25, 26] [25, 26] [25, 26] [25, 26] Thus, we have used different ammonium based ILs (Scheme 1) modified at the cationic moiety to investigate the hydrophobic effect on refolding of the thermally unfolded BSA. We tried to describe the impact of ILs at different concentrations ($2*10^{-6}$ – 2 M) on protein refolding after thermal denaturation by using experimental and computational studies. As well as, the impact of ILs on the structure and activity of the protein has been studied. Moreover, a docking study was used to investigate the possible binding sites of the ILs on BSA protein.

## Materials and methods

### Materials

BSA (Product No- A2153) was purchased from Sigma-Aldrich. The protein was used as such received without any further purification. 8-Anilino-1-naphthalenesulfonic acid ammonium salt (Product No-10417) and 4-Nitrophenyl acetate (esterase substrate) were purchased from Sigma-Aldrich and all other chemical required for IL synthesis were purchased from different commercial sources and were used without purification. 10 mM phosphate buffer was prepared using 18 MΩ.cm Milli-Q water (Millipore, Bedford, MA) and was used to prepare the samples throughout the work.

IL synthesis - Triethylalkylammonium bromides were prepared by the alkylation of triethylamine (100 mmol) with corresponding alkyl halide i.e. ethyl bromide, N-butyl bromide, N-hexyl bromide (100 mmol) in solvent acetonitrile using previously reported study.[27] The reaction mixture was stirred vigorously at a temperature of 75 $^0$C for 12 h in an oil bath, which was fitted with a reflux condenser. The solid product was washed thoroughly with hexane, filtered and dried under vacuum at 75 $^0$C for 6 h to obtain the pure ILs.

### Methods

*Circular Dichroism measurements:* The secondary and tertiary structures of BSA were monitored using JASCO-1500 CD spectrophotometer using a 0.1 cm path length cuvette. The scan speed (100 nm/min) was fixed with a response time of 1 s and 1 nm bandwidth. The protein's concentration was maintained at 2 μM & 100 μM for far-UV & near-UV studies respectively and IL concentration was varied from $2*10^{-6}$ M to 2 M and each spectrum was collected by averaging two spectra. Each sample spectrum was obtained by subtracting the appropriate background (without protein) from the experimental protein spectrum.

For thermal unfolding and refolding studies, each sample was subjected to a heating cycle of 25-90-25 $^0$C at a rate of 10 $^0$C/min.

*Molecular dynamic simulation:* The molecular dynamic simulations for BSA in IL (N2, N4, N6) and aqueous medium were performed by GROMACS 5.0.4[28] package using the GROMOS96 53a6[29] force field. Force field parameters for the N2, N4, and N6 ILs were generated using the PRODRG 2.5 server.[30] These systems were prepared with the protein which was further solvated in cubic boxes containing 30640, 28655 and 26303 simple point charge (SPC)[31] water molecules and 2 M concentration of N2, N4, and N6 ILs respectively. The aqueous system was solvated with 41934 SPC water molecules. All these

View Article Online
DOI: 10.1039/C7NJ02900D



systems were embedded in the cubic boxes where the protein was kept at center and at least 1.0 nm from the edge and the periodic boundary conditions were also employed. To remove the steric clash, the aqueous and IL systems were first energy minimized for 100 ps using the steepest descent method keeping the protein heavy atoms restrained with force constant of 1000 kJ $mol^{-1}$ $nm^{-2}$. Finally, the systems were optimized for 500 ps without heavy atoms restrained. The LINCS algorithm was utilized to constrain bond lengths, allowing the application of 2 fs time step.[32] The equation of motion was integrated with Verlet algorithm[33] utilizing different time steps. The electrostatic force was calculated through the particle mesh Ewald method (PME).[34] Van der Waals interactions were calculated by applying a 1nm cutoff. All the temperatures were kept with V-rescale temperature coupling during the simulation process.[35] These systems were equilibrated at 25° C under NVT condition and 1 bar pressure using Parrinello-Rahman barostat[36] in NPT for 1 ns. Finally, 10 ns MD simulations were performed for all the systems. The final conformation was taken and equilibrated at 90° C temperature under NVT condition and 1 bar pressure using Parrinello-Rahman barostat in NPT for 1 ns and 10 ns MD simulation performed. Again the last conformation was taken and equilibrated with the temperature at 25 °C under NVT condition and 1 bar pressure using Parrinello-Rahman barostat in NPT for 1 ns and 10 ns MD simulation performed. The analysis was performed using various GROMACS inbuilt programs and the graphs were plotted using Grace.

*Fluorescence measurements:* Synchronous fluorescence spectra were obtained in the range of 200 to 600 nm by simultaneously scanning the excitation and emission monochromator of the spectrofluorometer with two different $\Delta\lambda$ values (15 and 60 nm). For measurements, 2 μM protein solution was used. The width of the excitation and emission slit was set to 3 and 3 nm, respectively.

*8-Anilino-1-naphthalenesulfonic Acid (ANS) Fluorescence Measurements*: Fluorescence of ANS was performed using Fluoromax-4P with excitation at 370 nm, and emission was recorded between 400 to 600 nm using the same fluorescence spectroscopy. For measurements, 2 μM BSA solution and 10 μM ANS was used. The width of the excitation and emission slit was set to 3 and 3 nm, respectively.

*Time-resolved fluorescence measurements:* A time correlated single-photon counting (TCSPC) spectrometer (Edinburgh, OB920) instrument was employed to measure the fluorescence lifetime of Trp residues of BSA. The light source was diode laser excited at 295 nm. Time-resolved fluorescence decay profiles were analyzed by nonlinear least squares iteration procedures using F900 decay analysis software. The quality of the fit is assessed by the chi-square ($\chi 2$) values and distribution of residuals. The protein concentration was fixed at 2 μM and IL concentration was varied from 0 to 2 M.

*Esterase-like Activity Assay:* The esterase-like activity of BSA has been exploited to investigate the effect of ILs on the functionality of the protein. Here, the action of BSA on p-nitrophenyl acetate (PNPA, that is, the substrate) has been investigated by monitoring the absorbance of the released product, p-nitrophenol, on a Cary-100 UV−vis spectrophotometer ($\lambda_{abs}$ = 400 nm, molar absorption coefficient ε = 17 700 $M^{-1}$ $cm^{-1}$). Briefly, the reaction conditions were maintained as [BSA] = 25.0 μM, [PNPA] = 50.0 μM, pH 7.40, and temperature = 37 °C (the temperature was kept constant at the given value by a recycling flow of water, with an accuracy of up to ±0.5 °C)

*Molecular docking*: Auto-dock Tools vina 1.5.4 program (which is much more efficient than Autodock 4) was used for the molecular docking between BSA and IL molecules.[37] The crystal structure of BSA (PDB, 3v03) was used in the docking. Polar hydrogens and partial atomic Kollman charges were assigned to the BSA using the default setting of autodock tools and blind docking was carried out. The center of the grid was fixed at the center of BSA (90.398 × 28.894 × 23.482) Å, and the grid dimension was set at (84 × 56 × 82) Å, which is enough to cover the whole protein. Chemdraw ultra 8 was used to create the structure of IL and the optimized structures were obtained from the Avogadro software[38] using MMFF94 forcefield[39]. For the IL, the gasteiger charges were computed by the default setting of Autodock tools. The results were analysed using the lowest energy conformation out of the 9 conformations produced. The Pymol software was used for visualization of the residues involved in binding.

View Article Online
DOI: 10.1039/C7NJ02900D



## Results and Discussion

### Thermal unfolding and refolding studies

### Circular dichroism spectra

Far and near UV CD measurements have been employed to illustrate the secondary and tertiary structure of folded as well as unfolded BSA. When the temperature is increased, BSA begins to denature along with the breaking of intra-protein hydrogen bonds which maintain its active conformation and the internalized hydrophobic core exposed to the surrounding medium. The secondary structural content was determined from the far-UV CD spectra between 190-250 nm. Specifically, α- helix percentages of BSA were calculated according to the previous studies (as BSA is a α-helical protein).[40]

**Table 1**. *α- helix percentage of BSA in IL medium

| Conc. | $2\times10^{-6}$ M | | | | $2\times10^{-5}$ M | | | | $2\times10^{-4}$ M | | | | $2\times10^{-3}$ M | | | |
|---|---|---|---|---|---|---|---|---|---|---|---|---|---|---|---|---|
| IL | Intial $25^0$C | $90^0$C | Final $25^0$C | % loss | Intial $25^0$C | $90^0$C | Final $25^0$C | % loss | Intial $25^0$C | $90^0$C | Final $25^0$C | % loss | Intial $25^0$C | $90^0$C | Final $25^0$C | % loss |
| N2 | 64 | 33 | 53 | 14 | 65 | 34 | 55 | 15 | 65 | 34 | 55 | 15 | 66 | 33 | 56 | 15 |
| N4 | 60 | 29 | 51 | 15 | 65 | 33 | 54 | 17 | 62 | 31 | 52 | 16 | 63 | 32 | 56 | 11 |
| N6 | 65 | 35 | 56 | 14 | 68 | 39 | 61 | 10 | 73 | 40 | 65 | 10 | 68 | 42 | 64 | 5 |
| Buffer | 63 | 31 | 54 | 15 | | | | | | | | | | | | |

$$*\alpha-\text{helix}(\%) = \frac{(-\text{MRE}_{208}-4000)}{33000-4000}\times 100, \text{ where MRE} = \frac{observed\ CD}{c_p n l 10}$$, [Cp is the molar concentration of the protein, n is the number of amino acid residues of the target protein, and l is the path length in cm (0.1)]

$$\%\ \text{loss} = \frac{\alpha-\text{helix of the native state}\ (Intial\ 25^0\text{C}) - \alpha-\text{helix of refolded state}\ (Final\ 25^0\text{C})}{\alpha-\text{helix of native state}} * 100$$

From Table 1, it is clear that BSA has 63% α- helicity in the buffer medium at 25 $^0$C which is in agreement with the previous reports.[41, 42] In the presence of the ILs (up to a concentration of $2*10^{-3}$ M) the α- helicity remains intact, which suggests that ILs do not disturb the native structure of BSA. But, in the presence of N6 IL, a marginal increase in helicity was observed. This may be because of the increase in the compactness of protein in this particular IL which was validated by the fluorescence experiments. The percentage of α- helicity of BSA decreased to 31 when the temperature was maintained at $90^0$C. On cooling the sample to room temperature, it was found that 15% of its α- helicity was lost. Table 1 shows that N2 and N4 have the same ability to refold the protein as was observed in buffer medium. N6 has a better refolding ability at concentrations, $2\times10^{-5}$ M, $2\times10^{-4}$ M and $2\times10^{-3}$ M. (Figures are provided in SI). Note that due to the generation of higher HT voltage beyond the concentration of $2\times10^{-3}$ M, the spectra become noisy. This prevents us to measure the secondary structural content of the protein at relatively higher concentrations.

In order to obtain the information on the tertiary structure of the protein in all ILs, we performed near UV CD measurements and the results are presented in figure 1. BSA tertiary structure is characterized by the presence of two minima at 261 and 268 nm. BSA contains 17 cystines, 27 phenylalanines (Phe), 20 tyrosines (Tyr) and 2 tryptophans (Trp).[43] It was reported that the cystine residue has a negative band at around 260 nm.[44] Phe residues also show weaker negative bands above 240 nm.[44] Therefore, the strong negative bands are attributed to the asymmetric environment around disulphide chromophores and phe residues.[26, 45-47] The environment around aromatic chromophores can be analysed by studying the region 270-300 nm.[45, 47, 48] From the results, it was observed that the ellipticity at 261 & 268 nm was not altered much in the presence of all ILs. It was also important to note that there was no significant change in ellipticity in the region 280-300 nm, which confirms no significant changes in the

View Article Online
DOI: 10.1039/C7NJ02900D



environment around aromatic residues. Upon heating to 90 $^0$C, the CD spectrum changes dramatically (Figure 1 and complete analysis provided in SI). The signal at 261 and 268 nm now increases rapidly. This comparatively featureless spectrum indicates that the protein is unfolded. The non-zero CD signal arises due to the disulfide bonds, which remain intact at elevated temperatures. This spectrum at high-temperature is essentially same as was obtained for BSA at 90 $^0$C in the absence of IL. Upon cooling to 25 $^0$C, in the presence of N4 (2 M) and N6 (0.02 M & 2 M), the CD spectrum is mostly consistent with that recorded prior to heating, suggesting that most parts of the BSA refolded correctly.

From the far UV studies, it was found that BSA is more stabilized in N6 as compared to N2 and N4. It is noteworthy to explore the hydrophobicity of ILs on stabilization of BSA. It is known well that more hydrophobic ammonium ILs are more viscous. Thus, N6 which is more hydrophobic has strong stabilizing effect against thermal denaturation. It is proposed that the high viscous ILs might affect the preferential hydration interactions. In addition, high viscous nature of ILs slows down the conformational changes in proteins and maintain its compact structure. Our results are in agreement with previous studies where high viscosity ILs showed stabilizing effect on biomolecules.[18, 49-51]

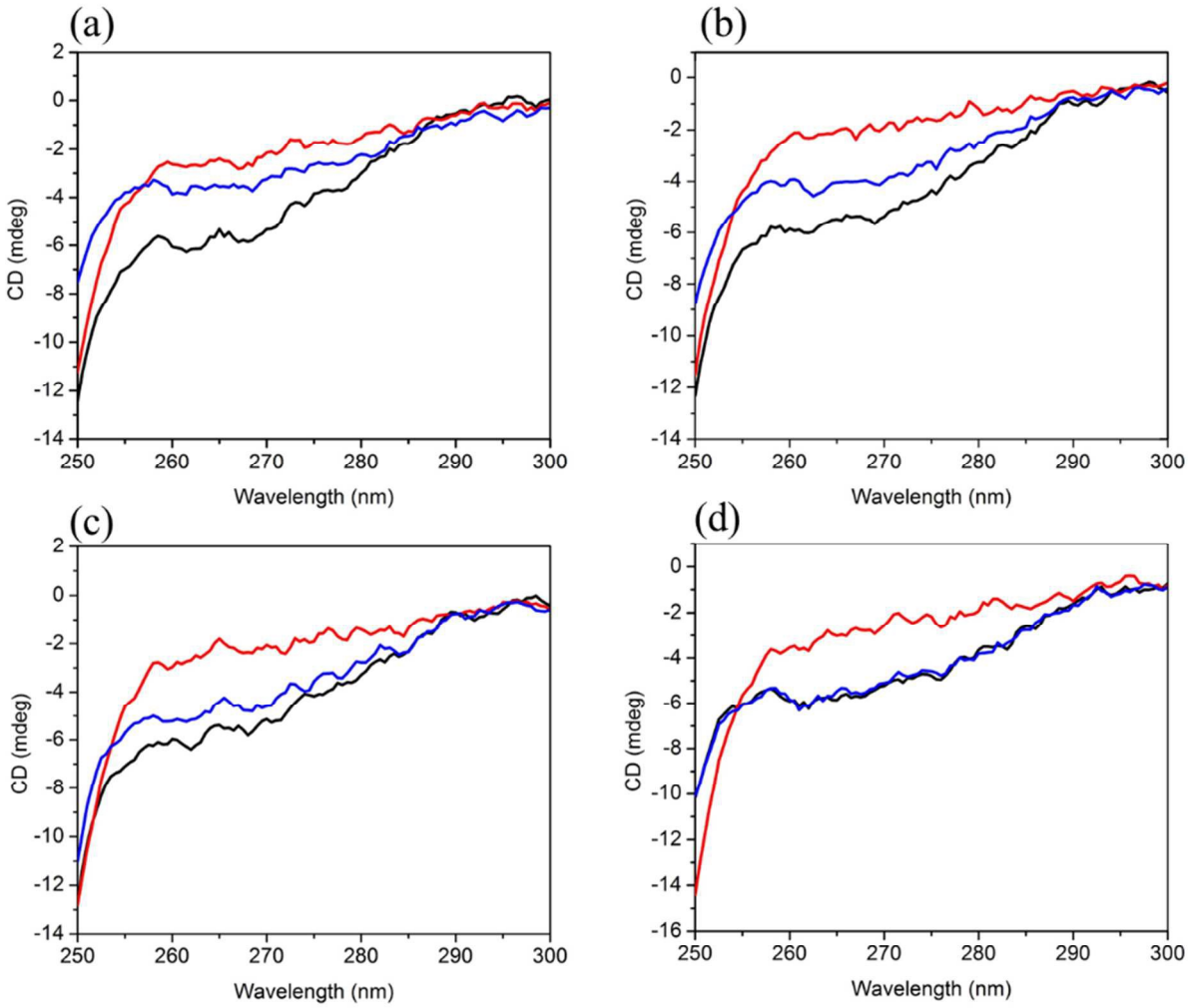


**Figure 1**. Near-UV CD spectra of thermal unfolding and refolding of BSA in buffer (a), N2 (b), N4 (c), and N6 (d). IL concentration is 2 M. [Colour code: Black-Native (25 $^0$C); Red-Unfolded (90 $^0$C); Blue-Refolded (25 $^0$C)]

The possible mechanism for stabilization could be due to the unfavorable interactions of ILs with protein surface. It is assumed that the exclusion of ILs from the protein's surface makes the protein more

View Article Online
DOI: 10.1039/C7NJ02900D



compact as observed in our results. The stabilization of protein's conformation by IL can be elucidated in terms of the interaction of ILs with the aqueous interface and the polypeptide chain of BSA. ILs are supposed to form a hydration layer with the water molecules around the protein. There are unspecific interactions with the surface of BSA, which eventually expelling the ILs from the surface of the protein.

When BSA is thermally denatured, the hydrophobic core of the protein is exposed outside. The hydrophobic core of BSA interacts favourably with the hydrophobic alkyl side chain of the ammonium ILs. These interactions are helpful in preventing protein aggregation and unfolding during denaturation process. When the protein solution is cooled down, the attached ammonium moieties desorb from the hydrophobic groups and protein is refolded. It is believed that short alkyl chain ammonium moieties may be strongly bound to the hydrophobic core of BSA, which prevents refolding of protein during cooling.

**Molecular dynamic simulation**

To support the experimental results, at first, we perform MD simulation of the protein (BSA) in aqueous and different IL medium at high temperature (90 $^0$C) for the duration of 10 ns. At the end of this simulation, the protein was found to be denatured. With this unfolded configuration, we carried out four separate MD simulations (in aqueous and presence of the three ILs) to visualize the effect of ILs on the structure of the protein at ambient conditions and the aqueous system was considered as baseline. IL concentration was kept constant at 2 M since the experimental results show better-refolding ability at this concentration. All these systems were equilibrated and 10 ns MD trajectories were generated. In the present case, we have explored the root-mean-square-fluctuations (RMSF) of Cα atoms in order to know the effect of ILs on thermal unfolding/refolding of BSA, because it could provide information on the flexible regions of the protein during the unfolding and refolding process. RMSF is mostly analyzed to get information on heterogeneity, local structural flexibility and thermal stability of macromolecules.[52-55] It can be seen from the average RMSF data of the amino acid residues of the protein that the regions of the protein containing residues 70-90, 170-180, 350-360, 490-500, 550-560 are found to be highly mobile in aqueous solution. Flexibility is mostly observed at the end of the helix and the sub domains where random coiling is present. Rigidity is found to be more in the sub domain IIA and IIIA compared to other sites. These observations are in agreement with the previous studies.[56, 57] Addition of ILs to the system decreases the RMSF values of the highly flexible regions which further depend on the type of IL. The RMSF values of the protein in an aqueous medium at 25 $^0$C reached the value 0.3 nm for all the flexible regions. It was observed that the RMSF values decreased in presence of ILs which follow the order of N2 > N4 > N6 (Figure 2). Note that the least values of RMSFs observed in presence of N6 which are found to be less than 0.2 nm. On increasing the temperature of the system, the RMSF values of both rigid and flexible regions intensified (Red lines in figure 2), which indicates the complete unfolding of the protein. Upon cooling the system to room temperature, the refolding process was noticed with the lowering of RMSF values (Green lines in figure 2). Moreover, the difference in RMSF values between native and refolded protein in presence of ILs was minimized compared to the aqueous medium and particularly, in the presence of N6, almost there was no difference. It suggests that N6 promotes refolding phenomena of BSA in a better way as compared to the other two ILs (N2 and N4).

As well as, the RMSD (root mean square deviation) values of the protein backbone atoms in the aqueous and IL mediums were calculated against the simulations time scale (0 -10 ns) which generally used to measure the conformational stability of proteins (Figure was provided in the SI). It is clear from the figure that the RMSD value of BSA in aqueous medium steadily increases from 0 to 4 ns, then the system reaches an equilibrium where it fluctuates around a value of 3.5 nm. For N2 medium, the RMSD values follow the same pattern as was observed for aqueous medium but the values were found to be higher than that of the aqueous medium after 4 ns. For N4 medium, the RMSD values were observed to be lower than the N2 medium and stabilized after 4 ns with an average value of 3.1 nm. Lowest values were noticed for N6 medium where the RMSD value was stabilized at an average value of 2 nm after 8 ns. Thus, it indicates that BSA becoming more stable in N6 medium which supports our RMSF results. Further to know the compactness of the system during simulation, $R_g$ (radius of gyration) values have been measured (Figure was provided in SI). $R_g$ is the measure of the mass-weighted root mean square

View Article Online
DOI: 10.1039/C7NJ02900D



distance of a collection of atoms from their common center of mass. It was observed that $R_g$ value of BSA in the aqueous medium is highly fluctuating during the entire simulation. In N2 medium, $R_g$ attains equilibrium after 4 ns, where the value was found to be fluctuating around 2.81 nm. Very few studies reported the $R_g$ value of BSA previously and our results are consistent with those results.[56, 57] The $R_g$ plots for N4 and N6 systems do not differ much in terms of the average value but it is worth noticing that the values for N6 system are lying below N4 system up to 6 ns and the N6 systems is stable during the entire simulation, whereas, the N4 system has values which are fluctuating more as compared to N6 system. By considering the overall effect, it is quite detectable that N4 and N6 system are stable and compact as compared to the N2 system but the aqueous medium with lower values after 5 ns cannot be just considered to compare with values of IL system because the values are highly varying throughout the simulation.

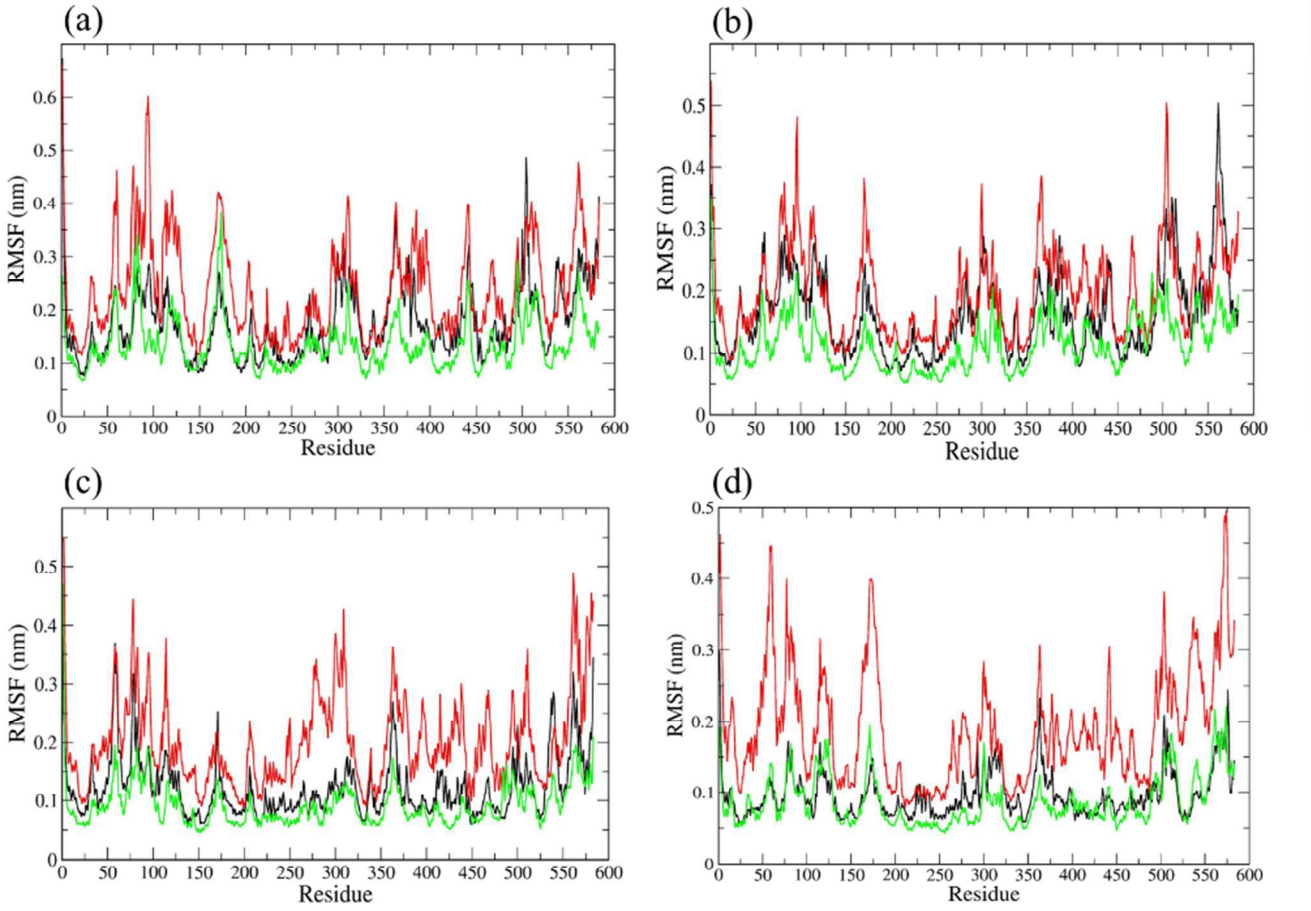


**Figure 2**. Average root-mean-square-fluctuations of thermal unfolding and refolding of BSA in buffer (a), N2 (b), N4 (c), and N6 (d). IL concentration is 2 M. [Colour code: Black-Native (25 $^0$C); Red-Unfolded (90 $^0$C); Green-Refolded (25 $^0$C)]

To explore the structural changes of BSA in IL medium, different fluorescence measurements were carried. BSA is a large protein (583 amino acid residues; ~66 kDa) composed of >60% α-helices with three homologous domains (I, II, and III). It has 20 Tyr residues and two Trp (Trp134 & Trp213) residues as intrinsic fluorophores (Scheme 1).[58]

**Synchronous fluorescence spectra analysis**

View Article Online
DOI: 10.1039/C7NJ02900D



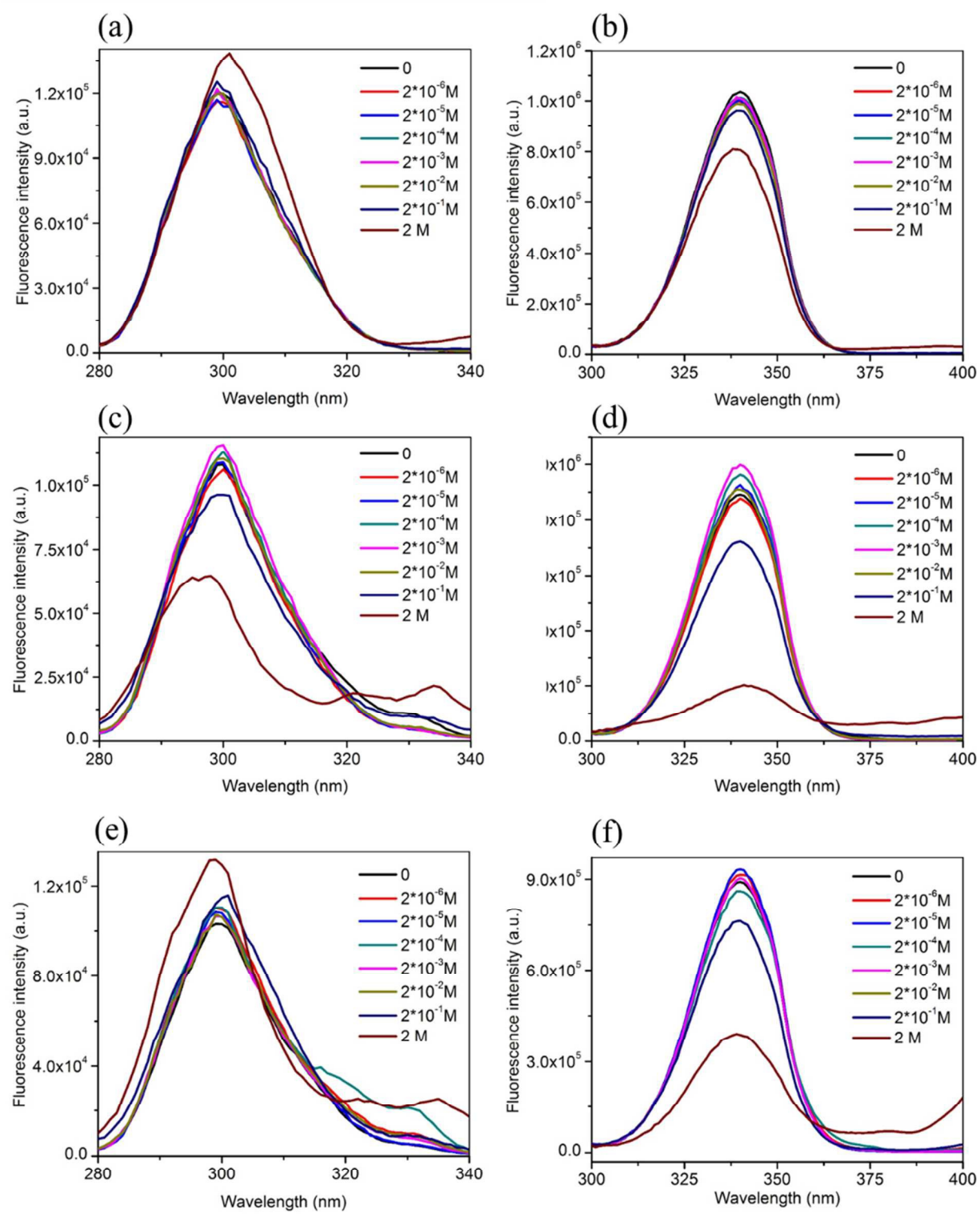


**Figure 3.** Synchronous fluorescence spectra of BSA in N2 (a & b), N4 (c & d), and N6 (e & f) with concentrations ($2*10^{-6}$, $2*10^{-5}$, $2*10^{-4}$, $2*10^{-3}$, $2*10^{-2}$, $2*10^{-1}$and 2 M). [$\Delta\lambda$=15 nm (a, c, e) and [$\Delta\lambda$=60 nm (b, d, f)]

View Article Online
DOI: 10.1039/C7NJ02900D



Synchronous fluorescence screening is useful to know the information of the local environment in the vicinity of fluorophore molecules. This method is more distinct in compared to the conventional excitation and emission spectra due to its spectral simplification, spectral bandwidth reduction and avoiding different perturbing effects.[59] This technique provides the characteristics information of the amino acid environment (particularly Tyr or Trp residues) by fixing the $\Delta\lambda$ at 15 or 60 nm.[60-62] In this method, the maximum emission wavelength is interrelated with environmental polarity around fluorophore molecules. To explore the structural change of BSA in IL medium, synchronous fluorescence spectra of BSA with various amounts of IL are recorded with $\Delta\lambda$ = 15 and 60 nm, as illustrated in Figure 3.

Figure 3 shows that the presence of ILs quenches the BSA fluorescence and large quenching is recorded when $\Delta\lambda$ = 60 nm is fixed as compared to $\Delta\lambda$ = 15 nm. This suggests that the ammonium moieties of the ILs are closer to the Trp residues than to the Tyr residues. The quenching indicates the interaction of ILs with protein molecule. But no shifting in the emission wavelength was observed which suggests that the Trp environment is not altered in the IL medium. Considering the effect when $\Delta\lambda$ = 15 nm, no significant quenching was observed rather high quantum yield noticed at higher concentration (2 M) in presence of N2 and N6. Up to concentration 0.2 M, no significant shift in emission wavelength observed. But at higher concentration (2 M), a slight red shift observed in presence of N2 but slight blue shift observed for N4 and N6. The reason for the blue shift could be due to increase in the hydrophobicity around the exposed Tyr residues. The addition of ILs can replace some of the water molecules present around BSA forming a preferential hydration layer along with water molecules. Thus, the replacement of water molecules by the hydrophobic ILs caused the hydrophobic environment around Tyr residues. In the case of N6, the increase in quantum yield suggests either the Tyr residues are far from the ammonium moieties or the protein becomes compact such that the residues are moving into the hydrophobic core of the proteins because of conformational changes in BSA.

**ANS Fluorescence spectra analysis**

ANS is an external fluorescent probe which is used to explore conformational states of proteins.[63] ANS exhibits higher fluorescence intensity when binds to the hydrophobic patches of proteins.[64] Thus, it supposes to show higher intensity when binds to the intermediate state of a protein compared to the native or fully unfolded state because hydrophobic patches are exposed in an intermediate state. The hydrophobic patches are inaccessible for ANS binding in native state and in the case of a completely unfolded state where the hydrophobic patches are disrupted. Figure 4 shows the ANS fluorescence in the presence of BSA at different concentrations of ILs. It was observed that ANS fluorescence gradual decreased with increase in the concentration from $2*10^{-3}$ to 2 M of each of the ILs. The diminished values of ANS fluorescence suggest the burial of hydrophobic patches. The complete unfolding can be ignored by considering the results observed from CD analysis. Therefore, we assume that the protein forms a compact structure where the hydrophobic patches are buried and inaccessible for ANS binding. The other reason for diminished values may be due to the affinity of ILs towards the ANS binding sites. With increasing IL concentration, more ANS molecules from the binding sites are replaced by IL, which finally leads to reduced values of the fluorescence intensities. In that context, we can accept that the protein must be in the native state or a non-native compact structure by considering the results obtained from the CD analysis and Simulation results.

View Article Online
DOI: 10.1039/C7NJ02900D



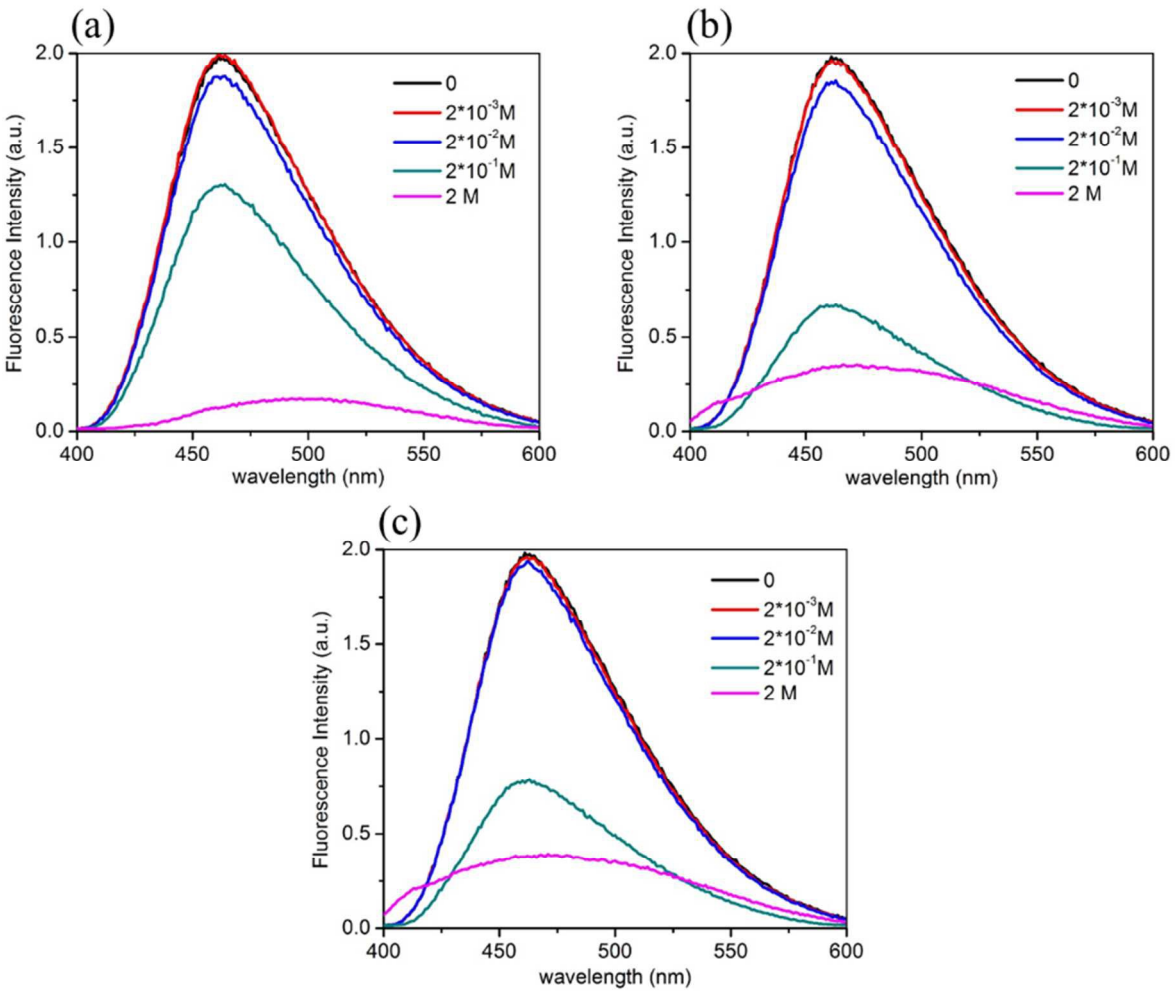


**Figure 4.** ANS fluorescence spectra in the presence of BSA and ILs with concentrations of ($2*10^{-3}$, $2*10^{-2}$, $2*10^{-1}$, 2 M); (a) N2, (b) N4, and (c) N6

**Fluorescence lifetime decay analysis**

Fluorescence lifetime provides valuable information on the local environment of fluorophore (Trp) residues and protein-IL interactions. It was observed that BSA exhibits a biexponential decay in both presence and absence of ILs (Figures provided in SI). The biexponential nature of Trp fluorescence decay can be explained on the basis of different environments around two Trp residues.[65, 66] But it is important to notice that Human serum albumin containing a single Trp residue also shows a biexponential decay.[67, 68] As well as, fluorescence decay of free Trp in aqueous solutions is biexponential due to the presence of rotational conformations (rotamers).[69-72] Therefore, it is not easy to assign the mechanistic models to the different components of multiexponential decay. In the present case, we prefer to use the average lifetime ($\tau_{avg}$) instead of emphasizing the individual decay constants to explore the effect of ILs on the structure of BSA. The average lifetime values for the biexponential decay were calculated using the equation 1. The lifetime decay data are given in Table 2.

$$\tau_{avg} = \alpha_1 \tau_1 + \alpha_2 \tau_2 \quad (1)$$

View Article Online
DOI: 10.1039/C7NJ02900D



**Table 2.** Fluorescence lifetime of BSA and BSA-IL systems

| IL | BSA in different medium | $\tau_1$(ns) | $\tau_2$(ns) | $\alpha_1$ | $\alpha_2$ | $\tau_{avg}$(ns) | $\chi^2$ |
|---|---|---|---|---|---|---|---|
| | Buffer | 3.22 | 6.79 | 0.217 | 0.783 | 6.02 | 1.02 |
| N2 | $2*10^{-3}$ M | 3.05 | 6.73 | 0.197 | 0.803 | 6.01 | 1.01 |
| | $2*10^{-2}$ M | 3.0 | 6.40 | 0.205 | 0.795 | 5.70 | 1.0 |
| | $2*10^{-1}$ M | 2.36 | 5.54 | 0.147 | 0.853 | 5.07 | 1.04 |
| | 2 M | 2.33 | 4.70 | 0.190 | 0.810 | 4.25 | 1.03 |
| N4 | $2*10^{-3}$ M | 3.19 | 6.80 | 0.200 | 0.80 | 6.08 | 1.027 |
| | $2*10^{-2}$ M | 2.76 | 6.30 | 0.167 | 0.833 | 5.71 | 1.015 |
| | $2*10^{-1}$ M | 2.56 | 5.63 | 0.176 | 0.824 | 5.09 | 1.018 |
| | 2 M | 2.12 | 4.65 | 0.244 | 0.756 | 4.03 | 1.01 |
| N6 | $2*10^{-3}$ M | 2.73 | 6.30 | 0.172 | 0.823 | 5.65 | 1.014 |
| | $2*10^{-2}$ M | 3.10 | 6.84 | 0.197 | 0.803 | 6.10 | 1.04 |
| | $2*10^{-1}$ M | 2.57 | 5.64 | 0.20 | 0.80 | 5.03 | 1.04 |
| | 2 M | 2.45 | 4.98 | 0.593 | 0.41 | 3.49 | 1.08 |

From the lifetime data (Table 1), the degree of exposure of Trp can be predicted. It was observed that the Trp lifetime decreases with increase in the concentration of ILs, which suggests the possibility of conformational changes in BSA structure. As a result of structural changes, the Trp-residues might be moving to a different environment relative to that present in native BSA. It is well known that Tyr, cysteine, positively charged histidine, and cystine are best quenchers in proteins.[73] Fluorescence lifetime gets affected by these quenching side chains when they are in proper orientation and proximity of indole ring. Thus, the diminished lifetime values suggest that the protein forms a compact structure by which the quenching ability of the nearby amino acids enhanced. These results are in agreement with ANS fluorescence results which revealed the burial of hydrophobic patches.

**Esterase like activity assay**

The impact of the ILs on the activity of BSA has been evaluated by monitoring the esterase-like activity of BSA. Here, the action of BSA on the p-nitrophenyl acetate (PNPA) substrate was investigated by monitoring the absorbance of the liberated product, p-nitrophenol ($\lambda_{abs}$ = 400 nm). The experimental details of the reaction conditions are mentioned in relative section. It was reported that the catalytic activity of BSA is exhibited by the reactive residue Tyr-411 present in subdomain IIIA with different catalytic cleavage mechanisms.[74] It is the first residue rapidly acetylated by PNPA.[75] Moreover, Lys-413 and 414 are also reacted with the substrate and rapidly acetylated.[46] When ligand molecules bind to the subdomain region which may interfere the catalytic activity of BSA. The influence of the interaction of the ILs on the activity of BSA was shown in figure 5 (kinetic study). The relative esterase-like activity of BSA in the presence of the different ILs with varying concentrations was investigated (Figure 6). Here, one unit of activity is defined as the amount of enzyme (BSA) required to liberate 1 μM of p-nitrophenol from the substrate (PNPA) per minute at 37 °C.

View Article Online
DOI: 10.1039/C7NJ02900D



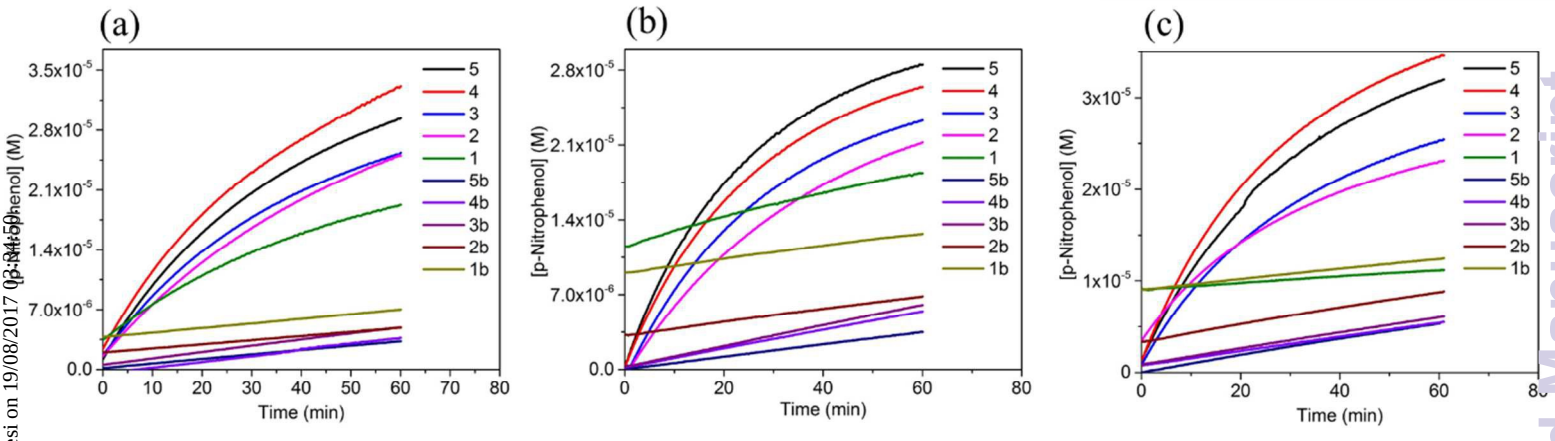


**Figure 5**. Representative kinetic profiles for the release of p-nitrophenol from the action of BSA and BSA-IL system on p-nitrophenyl acetate; (a) N2, (b) N4 and (c) N6 [notation representation, 5-BSA+buffer, 4- BSA+0.002M IL, 3-BSA+0.02M IL, 2-BSA+0.2M IL, 1-BSA+2M IL, 5b-buffer, 4b-0.002M IL, 3b-0.02M IL, 2b-0.2M IL and 1b-2M IL]

It is clear from the figure 6 that the esterase activity of BSA in not much influenced by the ILs at low concentration ($2*10^{-3}$M) rather a higher activity observed in the case of N2 and N6. But with an increase in the concentration of ILs, there was a gradual loss of activity observed and it was found to be higher in the case of N6 followed by N4. The outcome of the experiment shows that the protein maintains the esterase like activity (>60%) in presence of all studied ILs except in 2 M N6 IL, where a drastic loss of activity noticed. Though the spectroscopic and computational studies showed a native/non-native stable structure, the esterase like activity results appeared strange in the case of N6 IL. Molecular docking results reveal that the N4 and N6 IL bind to subdomain IIIA (discussed later). Since the reactive residues (responsible for esterase activity) present in that region, the binding of ILs may interfere with the catalytic activity of the protein. In presence of higher concentration of IL in the system, the ILs may compete with the PNPA for binding to the active site which could make the loss of the activity of the protein. It is clear from the kinetic study (figure 5b, c), where the free ILs (without protein) also exhibits higher activity as the protein. This suggests that the PNPA is probably staying in the IL medium (not bound to the protein) so that there was not much change in activity even after adding protein to the system (especially in 2M N4 and N6).

View Article Online
DOI: 10.1039/C7NJ02900D

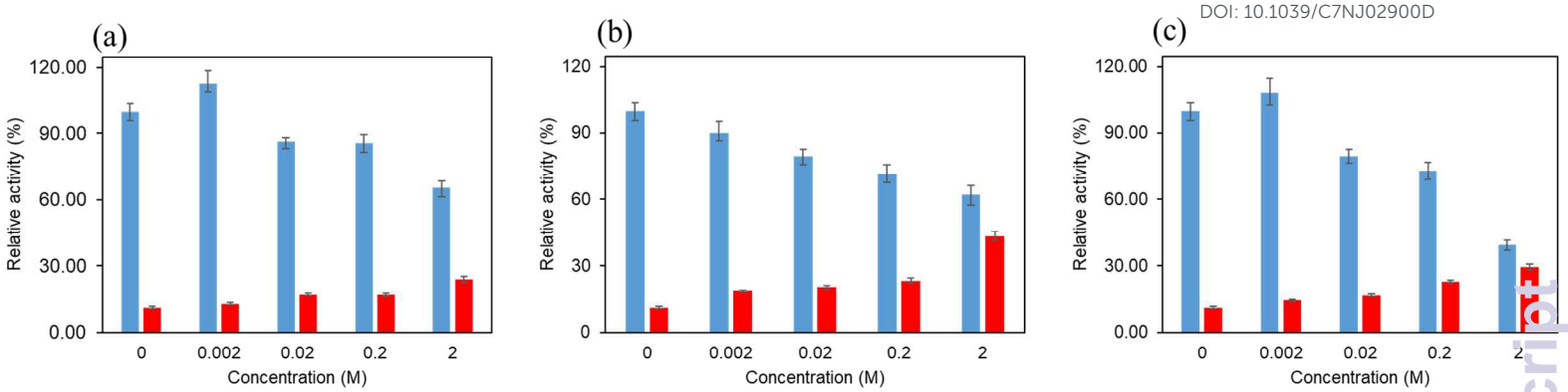


**Figure 6.** Modulation in relative esterase-like activity of BSA as a result of interaction with the ILs. The activity is monitored by following the release of p-nitrophenol from the action of BSA and BSA-IL system on p-nitrophenyl acetate; (a) N2, (b) N4 and (c) N6 [colour coding: Blue – Protein + IL & Red – IL(without protein)]; Error bars are found to be less than 6%.

**Molecular docking**

To investigate the possible binding sites of the IL in BSA, a molecular docking study (Auto dock vina[37]) was performed (Figure 7a-c). It was observed that there was no direct binding between BSA and IL. The nearby residues for the IL are as follows. (i) For N2, the residues are Leu-122, Tyr-160, Tyr-137, Leu-115, Lys-136 and Glu-140 (ii) For N4, the residues are Leu 189, Thr 190, Tyr 451, Ile-455 and Ser-428 and (iii) For N6, the residues are Ala-193, Leu-454, Ile-455, Ser-428, Lys-431, Tyr-451, and Thr-190. The binding free energies for N2, N4, and N6 are -4.0, -4.6, & -5.1 kcal $mol^{-1}$ respectively, which shows that strongest binding observed between BSA and N6. The only difference between all the ILs is the alkyl chain length, subsequently, it can be expected that the hydrophobicity of the IL majorly influences the binding interactions. The binding site of the ILs implies the influence of ILs on esterase activity of BSA. Since N4 and N6 bind to subdomain IIIA region, the impact on esterase like activity is expected to be more as the main catalytic residues present in that domain. Considering the overall activity assay results, the impact was found to be higher in presence of N4 and N6 as compared to N2 (binding site in subdomain IB) though the differences are marginal.

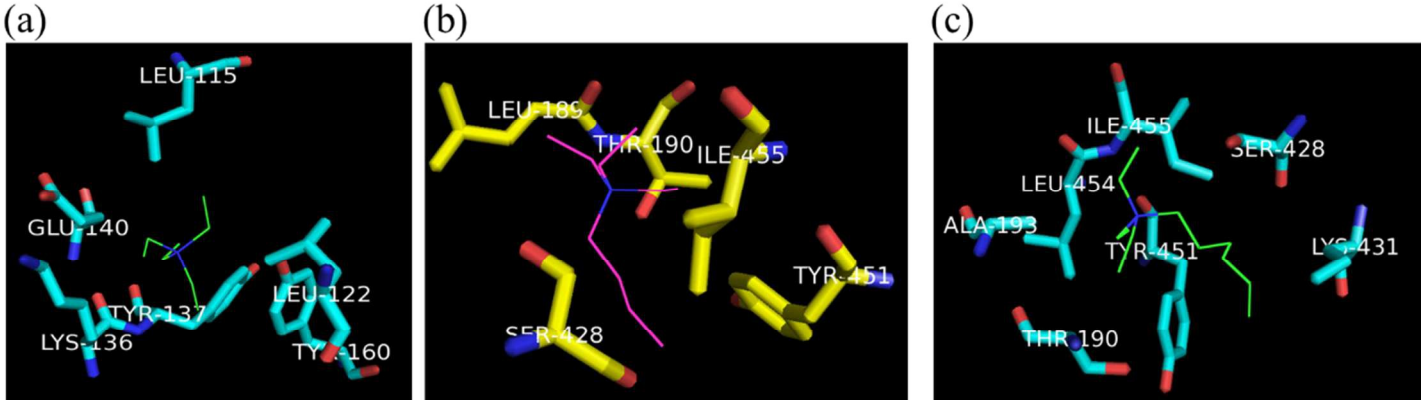


**Figure 7**. Molecular docking of BSA with (a) N2, (b) N4 and (c) N6

**Conclusion**

In summary, we found that all the studied ILs are biocompatible for BSA's structure. Among them, N6 has better efficiency in refolding the protein back to its native state after thermal denaturation, especially at higher concentrations. It can be concluded that the hydrophobicity of IL, as well as its concentration, plays a crucial role in thermal stabilization of BSA. However, further research with ILs varying the hydrophobicity of anion is required to know the effect of hydrophobicity of ILs on stabilization/destabilization of proteins. Our results illustrate the role of the alkyl group of ammonium

View Article Online
DOI: 10.1039/C7NJ02900D

based ILs is vital in determining the protein stability. Therefore, our research would be helpful in designing novel ILs which can provide stability to many other proteins.

**Acknowledgment**

Ministry of Human Resource Development, New Delhi is highly acknowledged for financial support. The authors are acknowledging ScfBio, IIT, Delhi for Supercomputing facility and the Department of Chemistry (NIT Rourkela) for the support in terms of the facility to carry out the experiments. Authors are also very thankful to Prof. Yixin Zhang and Prof.(Ms.) Madhurima Jana for their valuable suggestions.

**References**

1. T. Arakawat and S. N. Timasheff, *Biochemistry*, 1982, **21**, 6536-6544.
2. A. H. Doux, J. F. Willart, L. Paccou, Y. Guinet, F. Affouard, A. Lerbret and M. Descamps, *J. Phys. Chem. B*, 2009, **113**, 6119-6126.
3. S. Y. Gerlsma, *J. Biol. Chem.*, 1968, **243**, 957-961.
4. K. Fujita, D. R. MacFarlane and M. Forsyth, *Chem. comm.*, 2005, 4804-4806.
5. K. Rawat and H. B. Bohidar, *J. Phys. Chem. B*, 2012, **116**, 11065-11074.
6. J. V. Rodrigues, V. Prosinecki, I. Marrucho, L. P. N. Rebelo and C. M. Gomes, *Phys. Chem. Chem. Phys.*, 2011, **13**, 13614-13616.
7. T. Vasantha, P. Attri, P. Venkatesu and R. S. R. Devi, *J. Phys. Chem. B*, 2012, **116**, 11968-11978.
8. R. D. Roger and K. R. Seddon, *Science*, 2003, **302**, 792-793.
9. T. Welton, *Chem. Rev.*, 1999, **99**, 2071-2083.
10. R. Buchfink, A. Tischer, G. Patil, R. Rudolph and C. Lange, *J. Biotechnol.*, 2010, **150**, 64-72.
11. N. Byrne, L.-M. Wang, J.-P. Belieres and C. A. Angell, *Chem. comm.*, 2007 2714-2716.
12. C. Lange, G. Patil and R. Rudolph, *Protein Sci.*, 2005 **14**, 2693-2701.
13. H. Weingartner, C. Cabrele and C. Herrmann, *Phys. Chem. Chem. Phys.*, 2012, **14**, 415-426.
14. I. Jha and P. Venkatesu, *Phys. Chem. Chem. Phys.*, 2015, **17**, 20466-20484.
15. P. Attri, P. Venkatesu and A. Kumar, *Phys. Chem. Chem. Phys.*, 2011, **13** 2788-2796.
16. M. Bisht, A. Kumar and P. Venkatesu, *Phys. Chem. Chem. Phys.*, 2016, **18**, 12419-12422.
17. N. Byrne and C. A. Angell, *Chem. comm.*, 2009, 1046-1048.
18. J. P. Mann, A. McCluskey and R. Atkin, *Green Chem.*, 2009, **11** 785-792.
19. C. A. Summers and R. A. Flowers, *Protein Sci.*, 2000, **9**, 2001-2008.
20. P. Attri and P. Venkatesu, *Process Biochem.*, 2013, **48**, 462-470.
21. K. Fujita, D. R. MacFarlane, M. Forsyth, M. Yoshizawa-Fujita, K. Murata, N. Nakamura and H. Ohno, *Biomacromolecules*, 2007 **8**, 2080-2086.
22. P. Attri and P. Venkatesu, *J. Chem. Thermodyn.*, 2012, **52**, 78-88.
23. X. Yu, F. Zou, Y. Li, L. Lu, X. Huang and Y. Qu, *Int. J. Biol. Macromol.*, 2013, **56**, 62-68.
24. A. Kumar and P. Venkatesu, *RSC Adv.*, 2014, **4**, 4487-4499.
25. I. Jha, A. Kumar and P. Venkatesu, *J. Phys. Chem. B*, 2015, **119**, 8357−8368.
26. L. Satish, S. Millan and H. Sahoo, *Luminescence*, 2017, **32**, 695-705.
27. H. Li, G. Zhao, F. Liu and S. Zhang, *J. Chem. Eng. Data*, 2013, **58**, 1505−1515.
28. H. J. C. Berendsen, D. van der Spoel and R. van Drunen, *Comput. Phys. Commun.*, 1995, **91**, 43−56.
29. C. Oostenbrink, A. Villa, A. E. Mark and W. F. van Gunsteren, *J. Comput. Chem.*, 2004, **25**, 1656−1676.
30. A. W. Schüttelkopf and D. M. F. van Aalten, *Acta Crystallogr., Sect. D: Biol. Crystallogr.* , 2004, , **60**, 1355−1363.
31. H. J. C. Berendsen, J. P. M. Postma, W. F. van Gunsteren and J. Hermans, *Interaction Models for water in relation to protein hydration*, Springer Netherlands, 1981.
32. B. Hess, H. Bekker, H. J. C. Berendsen and J. G. E. M. Fraaije, *J. Comput. Chem.*, 1997, **18**, 1463−1472.
33. L. Verlet, *Phys. Rev.*, 1967, **159**, 98-103.

View Article Online
DOI: 10.1039/C7NJ02900D



34. O. K. Abou-Zied and O. I. K. Al-Shihi, *J. Am. Chem. Soc.*, 2008, **130**, 10793−10801.
35. G. Bussi, D. Donadio and M. Parrinello, *J. Chem. Phys.*, 2007, **126**, 014101.
36. M. Parrinello and A. Rahman, *J. Appl. Phys.*, 1981, **52**, 7182−7190.
37. O. Trott and A. J. Olson, *J. Comput. Chem.*, 2010, **31**, 455-461.
38. M. D. Hanwell, D. E. Curtis, D. C. Lonie, T. Vandermeersch, E. Zurek and G. R. Hutchison, *J. Cheminform.*, 2012, **4**, 17.
39. T. A. Halgren, *J. Comput. Chem.*, 1999, **20**, 720-729.
40. Y. Shu, M. Liu, S. Chen, X. Chen and J. Wang, *J. Phys. Chem. B*, 2011, **115**, 12306–12314.
41. A. Baral, L. Satish, D. P. Das, H. Sahoo and M. K. Ghosh, *New J. Chem.*, 2017, DOI: 10.1039/c7nj01227f.
42. L. Satish, S. Millan, S. Das, S. Jena and H. Sahoo, *J. Solution Chem.*, 2017, **46**, 831–848.
43. K. A. Majorek, P. J. Porebski, A. Dayal, M. D. Zimmerman, K. Jablonska, A. J. Stewart, M. Chruszcz and W. Minor, *Mol. Immunol.*, 2012, **52**, 174-182.
44. S. Beychok, *Science*, 1966, **154**, 1288-1299.
45. C. Sun, J. Yang, X. Wu, X. Huang, F. Wang and S. Liu, *Biophys. J.*, 2005 **88**, 3518–3524.
46. M. Dockal, D. C. Carter and F. Ruker, *J. Biol. Chem.*, 1999, **274**, 29303-29310.
47. M. Dockal, D. C. Carter and F. Ruker, *J. Biol. Chem.*, 2000, **275** 3042-3050
48. T. Chatterjee, A. Pal, S. Dey, B. K. Chatterjee and P. Chakrabarti, *PLoS One*, 2012, **7** e37468.
49. I. Jha, P. Attri and P. Venkatesu, *Phys. Chem. Chem. Phys.*, 2014, **16** 5514-5526.
50. P. Lozano, T. de Diego, J.-P. Guegan, M. Vaultier and J. L. Iborra, *Biotechnol. Bioeng.*, 2001, **75** 563-569.
51. P. Attri, I. Jha, E. H. Choi and P. Venkatesu, *Int. J. Biol. Macromol.*, 2014, **69**, 114-123.
52. M. Król, I. Roterman, B. Piekarska, L. Konieczny, J. Rybarska, B. Stopa and P. Spólnik, *Proteins.* , 2005, **59**, 545-554.
53. S. F. Sousa, P. A. Fernandes and M. J. Ramos, *Biorg. Med. Chem.*, 2009, **17**, 3369-3378.
54. J. Yin, D. Bowen and W. M. Southerland, *J. Mol. Graph. Model.*, 2006, **24**, 233-243.
55. J. Liu, H. Yu and Z. Shen, *J. Mol. Graph. Model.*, 2008, **27**, 529-535.
56. S. Jana, S. Dalapati, S. Ghosh and N. Guchhait, *J. Photochem. Photobiol. A: Chem.*, 2012, **231** 19- 27.
57. S. Jana, S. Ghosh, S. Dalapati and N. Guchhait, *Photochem. Photobiol. Sci.*, 2012, **11**, 323-332.
58. A. Bujacz, *Acta Crystallogr. Sect. D: Biol. Crystallogr.*, 2012, **68**, 1278-1289.
59. S. Millan, L. Satish, S. Kesh, Y. S. Chaudhary and H. Sahoo, *J. Photochem. Photobiol. B: Biol.*, 2016, **162**, 248–257.
60. S. Millan, L. Satish, K. Bera, B. Susrisweta, D. V. Singh and H. Sahoo, *J. Phys. Chem. B*, 2017, **121**, 1475-1484.
61. J. N. Miller, *Proceedings of the Analytical Division of the Chemical Society*, 1979, **16**, 203-208.
62. J. N. Miller, T. A. Ahmad and A. F. Fell, *Anal Proc* 1982, **19**, 37-41.
63. J. R. Lakowicz, *Kluwer Academic/Plenum Publishers: New York*, 1999.
64. O. K. Gasymov and B. J. Glasgow, *Biochimica et Biophysica Acta - Proteins and Proteomics*, 2007, **1774**, 403−411.
65. J. Tian, Y. Zhao, X. Liu and S. Zhao, *Luminescence*, 2009, **24**, 386-393.
66. B. Ojha and G. Das, *Chem. Phys. Lipids*, 2011, **164**, 144-150.
67. U. Anand, C. Jash and S. Mukherjee, *J. Phys. Chem. B*, 2010, **114**, 15839-15845.
68. E. L. Gelamo, C. H. Silva, H. Imasato and M. Tabak, *Biochim. Biophys. Acta*, 2002, **1594**, 84-99.
69. X. Shen and J. R. Knutson, *J. Phys. Chem. B*, 2001, **105**, 6260-6265.
70. A. G. Szabo and D. M. Rayner, *J. Am. Chem. Soc.*, 1980, **102**, 554-563.
71. Y. Engelborghs, *J. Fluoresc.*, 2003, **13**, 9-16.
72. H. Sahoo, D. Roccatano, A. Hennig and W. M. Nau, *Journal of American Chemical Soceity*, 2007, **129**, 9762-9772.
73. Y. Chen and M. D. Barkley, *Biochemistry*, 1998, **37**, 9976-9982.

View Article Online
DOI: 10.1039/C7NJ02900D

74. N. Moradi, M. R. Ashrafi-Kooshk, S. Ghobadi, M. Shahlaei and R. Khodarahmi, *J. Lumin.*, 2015, **160**, 351-361.
75. O. Lockridge, W. Xue, A. Gaydess, H. Grigoryan, S. J. Ding, L. M. Schopfer, S. H. Hinrichs and P. Masson, *J. Biol. Chem.*, 2008, **283**, 22582-22590.

View Article Online
DOI: 10.1039/C7NJ02900D

Experimental and theoretical evidences in support of the stabilizing effect of ammonium based ionic liquids on thermal unfolding/refolding of bovine serum albumin are provided in the article.